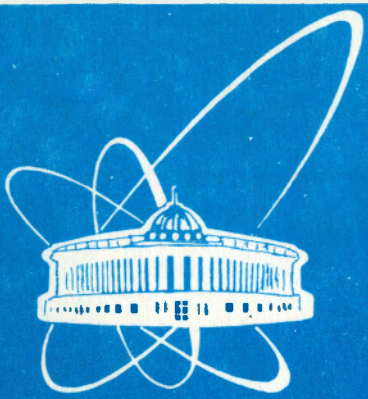

ОБЪЕДИНЕННЫЙ
ИНСТИТУТ
ЯДЕРНЫХ
ИССЛЕДОВАНИЙ

Дубна

E16-99-47

G.N.Timoshenko, V.P.Bamblevski, A.R.Krylov

THE TECHNIQUE OF MEASURING OF RELATIVISTIC PROTON ABSORBED DOSE IN THIN BIOLOGICAL SAMPLES

Submitted to «Nucleonika»

1999

Тимошенко Г.Н., Бамблевский В.П., Крылов А.Р. E16-99-47
Техника измерения поглощенной дозы релятивистских протонов в тонких биологических образцах

Изложена методика облучения образцов крови человека протонами с энергией 1 ГэВ. Эксперимент проводился с целью изучения хромосомных аберраций, индуцированных в лимфоцитах излучением, в диапазоне малых поглощенных доз. Рассмотрены вопросы расчета и измерения поглощенной дозы протонов с необходимой точностью в тонких образцах. Описаны методы формирования однородного пространственного распределения потока протонов, проходящих через образцы, и мониторирования протонного пучка.

Работа выполнена в Отделении радиационных и радиобиологических исследований ОИЯИ.

Препринт Объединенного института ядерных исследований. Дубна, 1999

Timoshenko G.N., Bamblevski V.P., Krylov A.R. E16-99-47
The Technique of Measuring of Relativistic Proton Absorbed Dose in Thin Biological Samples

The technique of blood samples irradiation by the 1 GeV protons is described. This experiment was carried out to study of chromosomic aberrations induced in human lymphocytes by the low absorbed doses. The problems of measurement and calculation of the absorbed dose of protons in thin samples with necessary precision are discussed. The method of forming the uniform spatial distribution of the proton flux that crossed the samples and the technique of the beam monitoring are presented.

The investigation has been performed at the Department of Radiation and Radiobiological Research, JINR.

Preprint of the Joint Institute for Nuclear Research. Dubna, 1999

INTRODUCTION

The experimental study of chromosomic aberrations induced in biological tissue by charged particles demands the absorbed dose measuring with accuracy of a few percents. In case of high energy of the accelerated particles it can be a sufficiently difficult problem. If the irradiated sample has a thickness enough to develop an inter-nuclear cascade the large number of secondary charged particles of various types will be generated inside the sample. At high energy of the beam particle the average multiplicity of the secondary particle generation becomes more than one. A big part of them escapes from the sample's volume and leaves within the sample portions of their energies only. On the other hand the secondary particles have a smaller energy than the beam particle but their ionizing energy losses are higher. The total amount of inelastic acts can be estimated in the first approximation as one percent along the matter thickness of one g/cm^2. The technique of calorimetric measuring is valid at the big mass of the sample and hasn't sufficient precision. The absorbed dose in the sample with not so great dimension can be obtained only by the calculation of deposited and received energies. The typical accuracy of the calculations by inter-nuclear cascade codes is more than few percents.

In case of the thin sample the problem of cascade particles is unimportant. However, some part of energy losses of primary particles will be carried off the sample volume by the secondary δ-electrons. The principal cause of the particle energy losses is ionization of matter atoms as the radiation losses of hadrons became appreciable only at energies higher several of GeV. The energy spectrum of δ-electrons falls down very rapidly but some of high-energy δ-electrons have ranges sufficient to escape from the volume /1/. The electrons with high energy usually move near the trajectory of the initial particle. The number of such electrons is scanty but their total energy can be significant if the particles irradiate the sample with the longitudinal size of several millimeters under normal direction to the front surface.

Thus, there is a certain range of the tissue thickness (from several millimeters up to several centimeters) where the energy absorbed in matter estimates with the most accuracy. As it is well known, the energy dose D absorbed in sample with thickness r is related in the first approximation with the charged particle flux F in the following way: Here it is supposed that:

$$F = \frac{D}{(dE/dx)_\infty} \qquad (1)$$

1) the particle energy doesn't change along the sample thickness (the case of relativistic particles);
2) the all-losses energy of particles is absorbed in tissue;
3) the sample is "transparent" for particles (the inelastic interactions are absent), i.e. the flux of particles doesn't change along the sample thickness;
4) the radiation losses of particles are absent.

If the material of the samples is homogeneous it is possible to write the balance of energies for every element Δx within the volume (see Fig.1):

$$E^{abs}_{\Delta x} = E^{all}_{\Delta x} + E^{in}_{\Delta x} - E^{out}_{\Delta x} \qquad (2)$$

where $E^{abs}_{\Delta x}$ – the energy absorbed in the Δx; $E^{all}_{\Delta x}$ – the energy lost by the charg particles along the Δx due to ionization; $E^{in}_{\Delta x}$ – the energy brought in the Δx by the high-energy δ-electrons from the previous volume; $E^{out}_{\Delta x}$ – the energy escaped from the Δx by the high-energy δ-electrons. Here it is supposed that the Δx thickness exceeds the range of higher-energy δ-electrons. The highest energy of δ-electrons from relativistic particle can reach 1 MeV and its range R_{max} in tissue is up to 5 mm. The δ-electrons entering in the Δx are generated within the layer w before the Δx. In this case the amount and $E^{in}_{\Delta x}$ of coming in the Δx δ-electrons are equal to the amount and $E^{out}_{\Delta x}$ of δ-electrons coming out from the w. Then, using these reasons we can overwrite the balance of energies (2):

$$E^{abs}_{\Delta x} = E^{all}_{\Delta x} + E^{out}_{w} - E^{out}_{\Delta x} = E^{all}_{\Delta x} - (E^{out}_{\Delta x} - E^{out}_{w}) \qquad (3)$$

Since the coming out from the Δx δ-electrons is also generated within the layer w of the element Δx, the difference in brackets is the energy coming out of the Δx by high-energy δ-electrons generated at thickness ($\Delta x - w$). If the thickness of the layer $w \geq R_{max}$. δ-electrons the incoming energy is always equal to the escaping energy, i.e. the electron equilibrium is maintained and the absorbed in the Δx dose energy can be obtained by (1). As the $w \leq R_{max}$ (the thin wall of a container, for example) the equilibrium is absent and the absorbed in the Δx dose energy will be always less than total ionization losses of the charged particles. The lost energy is:

$$E^{all}_{\Delta x} = (dE/dx)_\infty \cdot \Delta x \qquad (4)$$

The estimation of the coming out energy may be done with the help of any code for calculation of stopping power $(dE/dx)_L$, where L is the δ-electron's energy border. L can be found from the $R(L) = \Delta x - x$. Accordingly:

$$E^{out}_{\Delta x} - E^{out}_{w} = E^{out}_{\Delta x - w} = \int_w^{\Delta x} (dE/dx)_{L(x)} \cdot dx \qquad (5)$$

Here $L(x)$ - energy of δ-electron with range x. Then, the specific absorbed energy in the sample is:

$$dE^{abs}/dx = E^{abs}_{\Delta x}/\Delta x$$

DESCRIPTION

In accordance with the agreement between Biophysic Lab of NASA and JINR the irradiation of human blood lymphocytes was carried out at JINR synchrophasotron proton beam with energy of 1 GeV to study stable and unstable chromosomal aberrations. Before the irradiation the fresh blood was filled into the test-tubes of a tissue-equivalent plastic. The test-tube had the outer diameter 10.7 mm and the wall thickness w was 0.62 mm, hence the blood volume diameter was 9.5 mm. The blood sample contained nearly 2 cm^3 of blood. Taking the approximation of identical atomic composition of blood with tube's material and supposing their equivalence of tissue we estimated the portion of escaping energy. In order to produce the dose equal to 1Gy ($6{,}2415\times10^9$ MeV/g) in the tissue the flux of 1 GeV protons ($(dE/dx)_\infty = 2{,}2204$ MeV cm^2 g^{-1} /2/) must be $2{,}811\times10^9$ cm^{-2} in compliance with (1). The energy of δ-electron with the

range 0.62 mm is 280 keV. It is the minimum of necessary energy of δ-electrons (at the streamline of the beam) for their coming out from the deep Δx-w. Fig.2 presented the dependence of the lost energy portion of a proton $(dE/dx)_{L(x)}$ that was absorbed in tissue on coordinate x. The calculation was done with the code /3/. The right hatched area corresponds to the total proton energy escaping from Δx. The energy coming out from the zone $0 \div w$ (the left hatched area) is equal to the energy incoming to the Δx from the wall of the tube. The absorbed in Δx energy finds by the subtraction the square of hatched area from the square $(dE/dx)_{\square} \cdot \Delta x$. The hatched area in our case was 1.41% of the total energy and the average effective dE/dx along the sample was 2.181 MeV·cm^2·g^{-1}. In fact this result was even bigger due to the angular distribution of high-energy δ-electrons.

The next step of the real absorbed dose calculation was the estimation of the nuclear interaction of the beam's particles in the sample. In the sample the following charged particles with stopping power more than of the initial protons can be generated by inelastic interactions: low-energy protons, α-particles, recoil nuclei ($Z \sim 7$) and heavy fragments of nuclei ($Z \sim 4$). The total number of these interactions in the sample is less than 1% but their influence on the dose value is greater. In /4/ the contribution of secondary high LET (linear energy transfer) particles to the absorbed dose in CR-39 track detectors was measured. These experimental data were obtained at proton energies from 100 to 600 MeV. Assuming that the CR-39 material is equivalent to tissue (with accuracy of about 30%) and by the interpolation of the energies of the /2/ to 1 GeV the estimation of the absorbed dose augmentation in the blood sample was done. Its augmentation was found as 4.3%. Finally, the necessary proton flux across the sample at absorbed dose equal to 1 Gy was estimated as $(2.71 \pm 0.08) \times 10^9$ cm^{-2}. The error of this result was caused by the accuracy of the stopping power data mainly.

EXPERIMENTAL LAYOUT

The external proton beam from the accelerator transported into experimental hall and passed through the ionization chamber placed within the beam pipe. This current chamber is intended for total proton current monitoring. Then the beam was focused by two quadrupole magnetic lenses and went out into air from the vacuum pipe. The schematic view of the experimental setup is presented in Fig.3. The gap of this pipe called "Focus 3" is about 6 meters long and is used for experimental setup arrangement. Usually, the beam cross section in Focus 3 is near to 1.5 x 1cm^2. The main time structure of the beam is the following: the beam impulse width with time stretching is about 0.4 s and total cycle duration is 9.6 s at proton energy of 1 GeV.

The concentration of the lymphocytes along the vertical axis is different because of their fall-out within the tube. The shaking of the blood can't be tolerated. The three samples should be irradiated simultaniously. As a result, the uniform condition of the sample's set irradiation is necessary. To have nearly flat spatial distribution of protons in the area of the biological sample set, the beam was defocused on X, Y axes before Focus 3 by the magnetic lens. The tail of the defocused beam could interact with flange of the vacuum pipe and produced the secondary particles. This effect restricted the beam defocusing degree. The experimental setup was placed downstream Focus 3 just near the

multiwire proportional chamber standing out at the distance of 1,5 m from Focus 3 (Fig.3). This chamber is intended for relative XY spatial distribution measurement and has two coordinate planes with 20 × 20 cm^2 dimensions and 0.6 cm wire step.

BEAM MONITORING

For absolute monitoring of the number of protons interacting with the blood we used a small ionization chamber designed specially for these experiments. The first experiment with defocusing beam showed that the biologic sample size must be less 4÷5 cm^2 to guarantee good conditions of sample's irradiation and precise absorbed dose measurement. 3 test-tubes with blood were mounted side by side in the plane normally to the beam direction. The blood cross section was 3.6 x 3.0 cm^2 maximum. Consequently, the air-filled (under normal atmospheric pressure) ionization chamber for absolute monitoring of protons number had 4.2 × 4.2 cm^2 dimensions and the test-tube holder was mounted in 2.5 cm distance from the chamber center. The schematic design of the chamber is presented in Fig.4. The effective layer of air between electrodes was 6 mm thickness and high voltage bias was chosen equal to 850 V. These conditions caused a negligible level of ions recombination into the chamber. The construction of the chamber frame provided minimum amount of matter near the electrodes and biologic samples to avoid proton scattering processes. The chamber current through 2 meters cable leaked in the current-frequency converter with sensitivity 37.5 imp·nC^{-1}. The current-frequency converter calibration with direct current source showed that up to 10^5 imp·s^{-1} rate its integral nonlinearity was less than 0.2%.

The chamber thickness was 68 mg/cm^2 Al. The total thickness of matter between the vacuum pipe and the sample was approximately 0.5 g·cm^{-2}. As a result of it, about 0.5% of all protons could be scattered (elastic or inelastic manner) in space up to the sample. In practice the admixture of scattered particles across the sample irradiation area was negligible because of the smallness of necessary solid angles of the scattering.

The absolute calibration of the beam current chamber and our small chamber at real beam intensity range ($\approx 10^9 \div 10^{11}$ protons per cycle) was carried out with thin carbon-contained activation detectors. For calibration of the beam chamber the thin CH_2 detectors with diameter of 12 cm (slightly less than the outlet window of the proton pipe) were mounted on the pipe flange in three expositions. For calibration of the small ionization chamber we used the small CH_2 detectors (4.2 × 4.2 cm^2 dimensions) mounted directly after the chamber. These calibration procedures were repeated several times at different beam intensity. The detectors activation was measured by the gamma-spectrometer very thoroughly with account to the real source-detector geometry and self-absorption processes. The cross section of the $^{12}C(p,pn)^{11}C$ reaction was taken equal to 27 ± 1 mb. The resulting error of the number of protons per cm^{-2} measurements was estimated as 5÷6 % (including the reaction cross section error, methodological and statistical errors and taking into account the time structure of irradiation). We tested, with the same activation detectors, the exact linearity of the chamber readings depending on the beam intensity in the interval of $0.5 \times 10^9 \div 2 \times 10^{10}$ protons per cycle as well. Finally, the small chamber conversion factor was defined as 6.86×10^{-8} imp·proton^{-1}.

SPATIAL DISTRIBUTION OF THE PROTON FIELD

The absolute calibration of the small ionizing chamber gave one the possibility to define the average value of the proton flux density on 4.2 × 4.2 cm^2 square. As the biological sample's set had a smaller area, we needed to have nearly flat spatial distribution of protons inside this square (within ± 5% maximum). One should note, it restricted the achievable proton flux density and, consequently, increased the irradiation time. We optimized the beam defocusing adjustment by the multiwire proportional chamber standing before the samples and checked the spatial distribution by the matrix of thermoluminescence detectors (TLD) mounted direct behind the sample's place.

The current distributions from X and Y wires measured by the multiwire proportional chamber are shown in Fig. 5. The TLD-600 manufactured by HARSOW had 3.1 x 3.1 mm^2 sizes and 0.9 mm thickness. We used the matrix from 15×9=135 TLD spaced in 6 mm one after another (whole matrix dimensions are 8.8 (X) × 5.2 (Y) cm^2). To decrease of the proper TLD sensitivity dispersion the detectors graduation with ^{60}Co was carried out preliminarily. The individual correction coefficient for each detector was obtained and taken into account during data processing. The spatial distribution measured by the TLD matrix (in term of nC} is presented in Table 1. Within the biological sample's bounds (bold figures and shadow) the maximum TLD reading deviations from average value were +4.7 % and –6.5 %. The proton flux density deviations in this area were at least not more than TLD reading deviations. It allowed to calculate the absorbed dose of protons in samples with accuracy mainly limited by the proton flux measurement accuracy.

RESULT OF THE BLOOD SAMPLES IRRADIATION

After the proton beam defocusing we had 11.3 % of all beam protons, passing through the small chamber and biological samples. The correlation between the small chamber readings and activation detector readings were kept with accuracy of 1% during the samples irradiation. The other correlation between our chamber and the beam current chamber (within ± 2.1%) confirmed the stable beam position (without "walking") during the samples irradiation. The irradiation of the samples under the same absorbed dose were done in two stages (3 by 3 test-tubes per every dose exposition). The every exposition of the blood irradiation lasted from 10 to 15 cycles of the proton acceleration. The final results of the blood samples irradiation are presented in Table 2.

NUMBER OF PARTICLES CROSSED OVER THE LYMPHOCYTE

In assumption that the average cross section S of a lymphocyte equals to 7.8×10^{-5} cm^2 ($Ø \approx 10^{-3}$ cm) the probability of particle number n (0,1,2...) crossed S (described by the Poisson distribution) is:

$$P(n) = (a^n/n!)\cdot exp(-a)$$

where a is an average number of particles ($a = F\cdot S$); F – particle flux (cm^{-2}). For our case at the 1 Gy absorbed dose $a \approx 2\times10^5$. The interesting case is when the main number

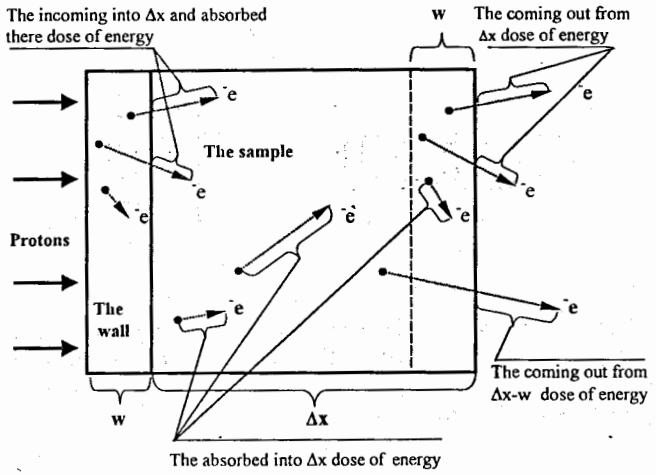

Fig.1. A schematic view of the processes dynamics of energy loss and absorption into the sample.

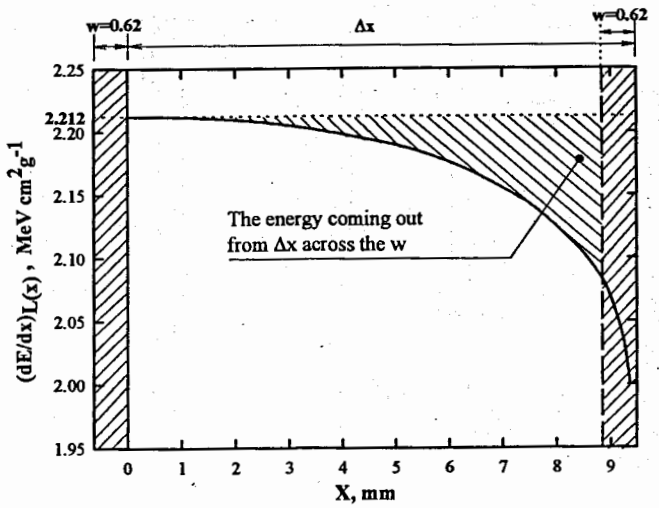

Fig.2. The $(dE/dx)_{L(x)}$ of the protons that crossed the sample in dependence on X. The left hatched area (the front wall of the tube) – the region from which the energy is transfering into the Δx. The right hatched area (the terminal part of the Δx that is equal to the w) – the region from which the energy is coming out from the Δx. These energies are equal. The upper hatched area – is the energy leaking out from the Δx-w region of the sample.

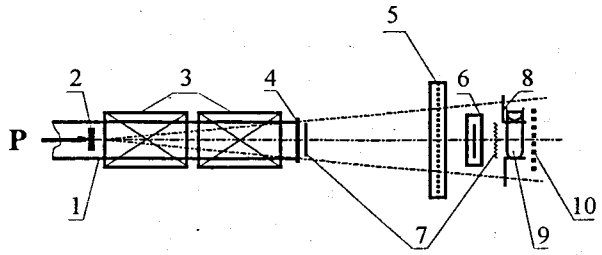

Fig.3. The experimental layout. 1- the vacuum pipe; 2 – the beam current chamber; 3 – the magnetic lenses; 4 – the flange of the pipe; 5 – the multiwire proportional chamber; 6 – the small ionisation chamber; 7 - the activation detectors; 8 – the sample's holder; 9 – the sample's set; 10 – the TLD matrix.

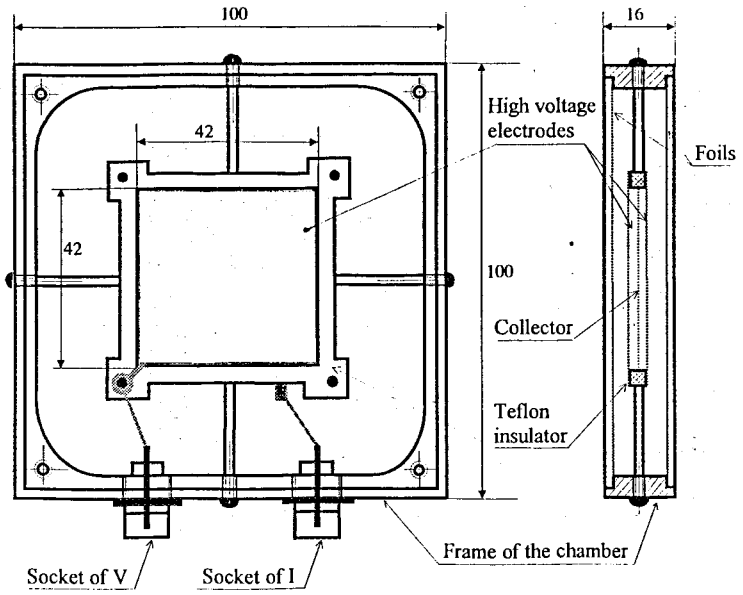

Fig.4. The design of the small ionisation chamber.

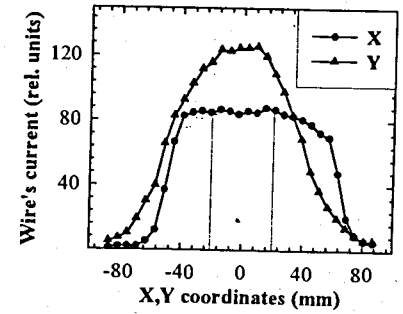

Fig.5. The typical spatial distributions of the wire currents of the multiwire proportional chamber. The sample's set dimensions are pointed by the thin lines.

Table 1. The part of the spatial distribution of the TLD matrix readings (in nC). The bold figures are corresponding to the sample's set area.

231,3	227,5	232,5	234,2	232,7	236,5	234,2	236,5	235,0	229,5	223,0
266,3	267,0	277,6	277,4	269,3	266,1	269,5	265,3	269,5	262,6	254,6
291,2	291,2	287,1	**300,2**	**288,8**	**286,5**	**297,0**	**292,6**	284,1	280,4	273,6
307,2	302,1	305,8	**312,4**	**309,5**	**306,5**	**304,3**	**302,4**	297,9	291,8	288,9
303,7	306,3	312,6	**320,1**	**316,7**	**321,2**	**315,4**	**300,2**	309,5	297,8	285,9
304,9	310,2	317,1	**319,3**	**313,2**	**316,2**	**300,6**	**309,0**	304,1	297,9	298,4
297,8	304,9	309,7	**311,4**	**306,0**	**311,5**	**305,9**	**301,4**	304,3	290,2	291,1
290,4	288,0	286,7	293,9	288,9	284,7	283,4	291,1	287,3	274,6	275,3
259,9	253,1	259,6	261,2	263,0	258,4	263,4	264,2	257,2	252,7	253,9

Table 2. The result of the blood samples irradiation.

The 1-st irradiation dose (Gy)	The 2-nd irradiation dose (Gy)	The average dose of blood mixture (Gy)
3.615	3.615	3.615
2.695	2.700	2.698±0.1%
1.605	1.625	1.615±0.6%
1.055	1.030	1.043±2.4%
0.543	0.535	0.539±0.9%
0.270	0.275	0.272±0.8%
0.144	0.146	0.145±1.0%

of lymphocytes are crossed over by one proton only (a = 0.5÷1.0). It is realized at absorbed dose of protons nearly to 0.2÷0.5 mGy. The ionization and activation methods are insensitive at this proton beam current but the scintillation counter can have a significant miscounts due to beam timing structure. Therefore such experiment needs a precise technique for dose measurement.

ACKNOWLEDGMENTS

The authors would like to thank Professor E.Krasavin and Dr. T.C.Yang. They are also grateful to Dr. V.Aleinikov , Dr. M.Komoshkov, Dr. R.Govorun and Dr. S. Novikov for their help in the experiment and useful discussion of the problem.

REFERENCES

1. Medvedev M.N. The scintillation detectors. Moscow, Atomizdat, 1977.
2. Nuclear Science Series. Report 39. National Academy of Science-National Research Council. Publication 1133. Washinghton. D.C., 1964.
3. Krylov A.R., Henniger Ju. ReportJINR. B1-11-86-386, Dubna, 1986.
4. V.E.Dudkin, F.Spurny. In Proc. of the 9th International Congress on Radiation Protection (April 1996, Vienna, Austria), v.2, pp.250-253.